

# Experimental Results on the Diffractive Production of Light Vector Mesons

James A. Crittenden ‡  
(for the H1 and ZEUS collaborations)

Deutsches Elektronen-Synchrotron, Notkestraße 85, 22603 Hamburg

**Abstract.** We discuss results on the diffractive production of the vector mesons  $\rho^0$ ,  $\phi$  and  $\omega$  reported by the H1 and ZEUS collaborations at HERA. Unique to such studies is the experimental accessibility to the polarization of the vector mesons and hence to the spin-density matrix elements arising in vacuum-exchange processes. We emphasize the relation between the observed dependence on momentum transfer and the polarization state of the vector meson. The diffractive nature of the production mechanism is investigated via extraction of the Pomeron trajectory at high  $Q^2$ . Flavor symmetry is observed in the  $\phi/\rho^0$  ratios in the same region of momentum transfer where the power-law scaling becomes similar. The multivariable helicity analyses impose stringent constraints on models for the vacuum-exchange production mechanism. Semi-exclusive photoproduction of transverse  $\rho^0$  and  $\phi$  mesons at momentum transfers far exceeding their mass scale exhibit a hard scaling behavior which appears to violate the QCD helicity selection rules in a two-gluon exchange model.

Contributed to the proceedings of the Ringberg Workshop on New Trends in HERA Physics 2001, 17–22 June 2001, Ringberg Castle, Tegernsee, Germany.

‡ On leave from Phys. Inst. Bonn, Nußallee 12, 53115 Bonn

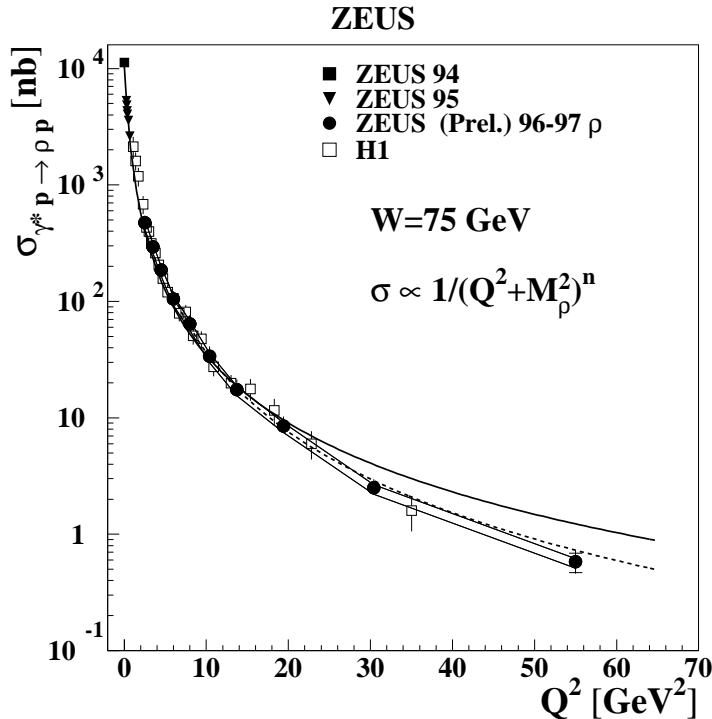
## 1. Introduction

Investigations of the exclusive production of vector mesons in electron-proton interactions by the H1 and ZEUS collaborations at HERA have yielded detailed information on vacuum-exchange dynamics, since the high flux of real and virtual photons from the electron beam provides a means of investigating such processes with high precision. The particular interest in the light vector mesons  $\rho^0$ ,  $\phi$  and  $\omega$  lies in the opportunity to reach kinematic regions of momentum transfer in which effects of binding are small and the fundamental scaling properties of the underlying vacuum-exchange process are revealed. In contrast to studies of inclusive processes, decay-angle analyses in exclusive and semi-exclusive processes yield detailed information on the spin-density matrix, i.e. the helicity-transfer characteristics of the production mechanism. Since these are related on very general theoretical grounds to the scaling properties in field theoretical descriptions [1, 2], stringent constraints on the phenomenological interpretation of strong vacuum-exchange mechanisms are obtained. In recent years, much theoretical work has been done on such interpretations, both for vector-meson electroproduction at high photon virtuality [3, 4], and for photoproduction at high momentum transfer [5–7].

This report concerns recent results on elastic  $\rho^0$  electroproduction from longitudinal and transverse virtual photons, including a Regge analysis at high  $Q^2$ , investigations of the dependence of the spin-density matrix elements on proton dissociation and the momentum transferred to the proton, as well as scaling and helicity-transfer properties of  $\rho^0$  and  $\phi$  photoproduction at high momentum transfer. The results address quantitatively a variety of theoretical concerns. By comparing the properties of the photon/vector-meson transition for elastic electroproduction to those for the proton-dissociative process, one tests the interpretation of the process as diffraction, since any difference implies a correlation between the photon/vector-meson and the hadronic vertices. Any  $Q^2$  dependence in an extracted Regge trajectory challenges a canonical assumption of fixed poles in Regge theory. The dependence of the forward cross sections on  $Q^2$  confront recent QCD descriptions of diffractive processes which predict asymptotic dominance of the production of longitudinal vector mesons from longitudinal virtual photons, with a  $Q^{-6}$  dependence modified by the  $Q^2$  dependence in the gluon density and in the strong coupling. The transverse cross section is expected to be suppressed by a factor of  $Q^2$ , though corrections due to the endpoints of the quark momentum distributions in the meson mitigate this expectation. A related line of argument has been proposed to predict the dominance of longitudinal vector mesons at high  $|t|$  in diffractive photoproduction, where  $t$  is the square of the momentum transferred to the proton. Again, production of transverse vector mesons is expected to be suppressed by a factor of  $t$ , resulting in a prediction of  $d\sigma/dt \propto (-t)^{-4}$ , modified by the  $t$  dependence in the gluon density and in the strong coupling. These helicity selection rules in the dependence on momentum transfer are straightforward consequences of the two-gluon model for diffractive processes [8].

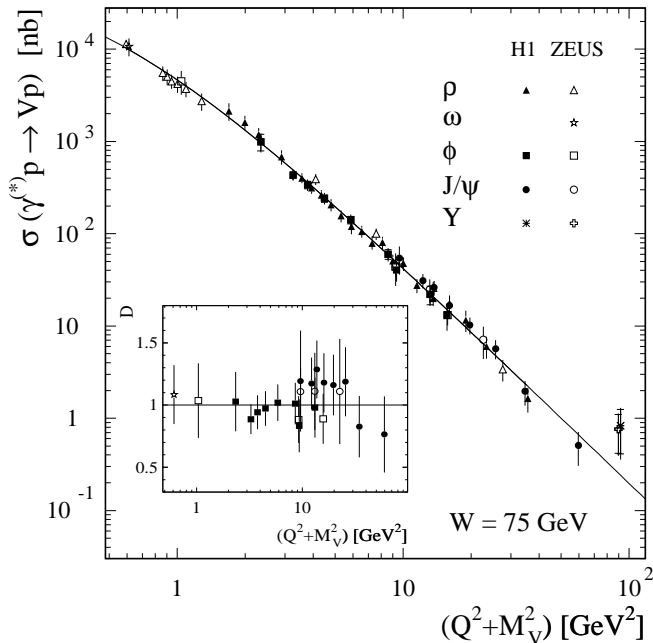
## 2. Scaling laws and helicity selection in vector-meson electroproduction

Figure 1 shows the recently obtained  $Q^2$  dependence of the total  $\rho^0$  elastic cross section presented by the ZEUS collaboration [9]. A fit to the form  $(Q^2 + M_\rho^2)^{-n}$  shows that



**Figure 1.** Elastic  $\rho^0$  electroproduction cross section as a function of  $Q^2$ . The lines show the result of fits to the form  $(Q^2 + M_\rho^2)^{-n}$ . The solid line indicates the result of the fit to all data points, while the dashed line is the result restricted to the points at  $Q^2 \geq 5 \text{ GeV}^2$ . Also indicated is an additional normalization uncertainty associated with the subtraction of the proton-dissociative background.

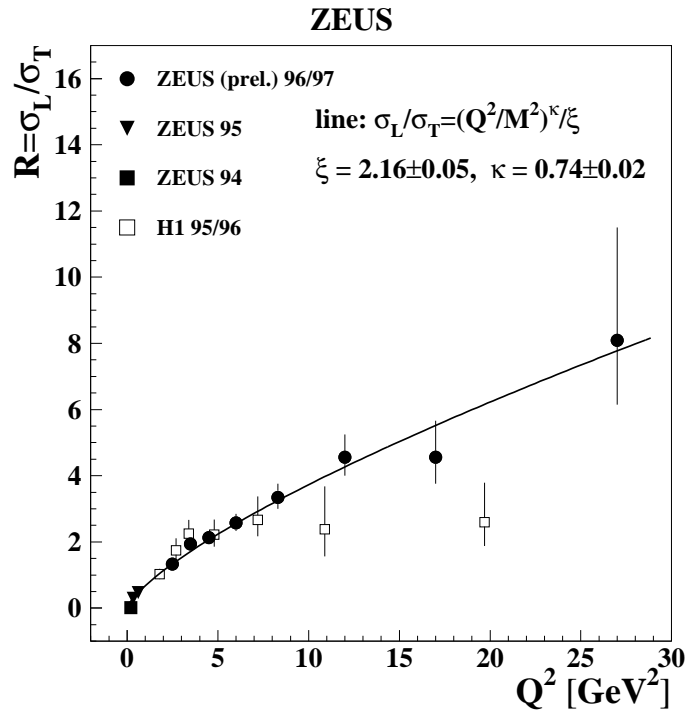
the power  $n$  varies with the lower bound on  $Q^2$  chosen for the fit. For lower bounds greater than  $5 \text{ GeV}^2$ , the fit is statistically consistent with a power of  $2.36 \pm 0.04$ . The H1 collaboration has remarked upon the scaling of the total cross section, pointing out that the  $\phi$  and  $J/\psi$  cross sections exhibit scaling behavior remarkably similar to that for the  $\rho^0$  when weighted with normalization factors corresponding to the quark-charge content of the meson, as shown in Fig. 2 [10]. However, each of the above observations is difficult to interpret phenomenologically, since the contributions from longitudinal and transverse photons are expected to scale differently, and the relative contributions are known to vary rapidly with  $Q^2$ , as shown in Fig. 3 [9]. This measurement of the ratio  $R = \sigma_L/\sigma_T$  allowed extraction of the scaling properties of  $\sigma_L$  and  $\sigma_T$  separately, as shown in Fig. 4 [11]. The separation of the scaling properties of the cross sections for longitudinal and transverse photons was obtained by analysis of the polar decay-angle distribution. The hard scaling behavior is impressive, since the longitudinal cross section is even harder than a point-like-scattering (Rutherford) cross section. In the context of QCD calculations which model vacuum exchange as the exchange of a color-neutral



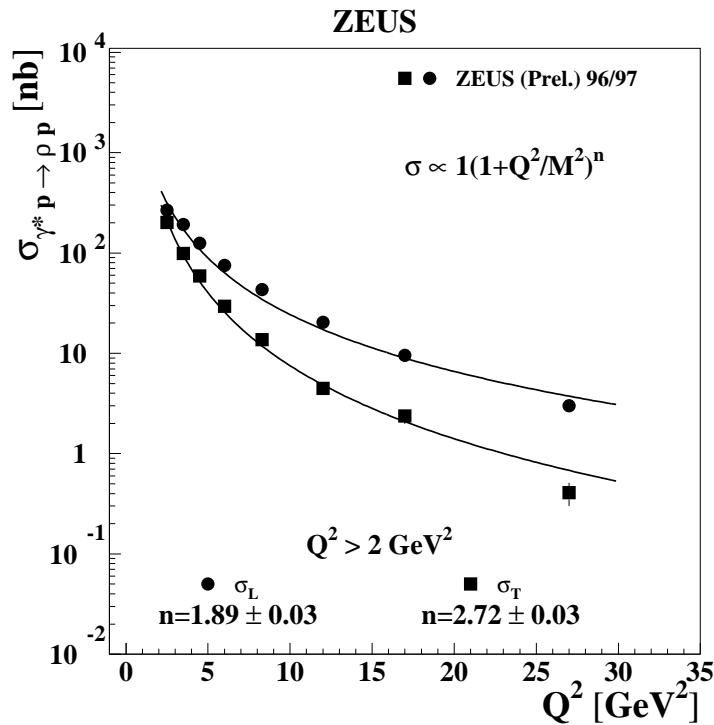
**Figure 2.** Elastic  $\rho^0$  electroproduction cross section as a function of  $(Q^2 + M_V^2)$  for  $V = \rho^0, \phi, \omega, J/\psi$  and  $\Upsilon$ , scaled according to the proportions 9:2:1:8:2, which correspond to the quark-charge content of the vector mesons. The error bars indicate the quadratic sum of statistical and systematic uncertainties. The curve indicates the result of a fit to the ZEUS and H1  $\rho^0$  data. The ratio  $D$  of the  $\phi$ ,  $\omega$  and  $J/\psi$  cross sections to the fit result is shown in the inset.

pair of gluons, this indicates that the  $Q^2$  dependence of the square of the gluon density compensates the leading  $Q^{-6}$  behavior by more than a factor of  $Q^2$ . Also remarkable is the hard behavior of the transverse cross section, which encourages a leading-order field theoretical interpretation as well. In the case of the production of transverse vector mesons, however, the QCD calculation is complicated by contributions arising from the endpoints of the quark momentum distribution in the vector meson [4], resulting in the necessity for modelling non-perturbative effects [12]. It has been experimentally established that the spin-flip contributions are rather small ( $\simeq 10\%$ ) [13], so the observed  $Q^2$  dependences in the cross sections for longitudinal and transverse photons are each determined by the helicity-conserving amplitudes to a good approximation.

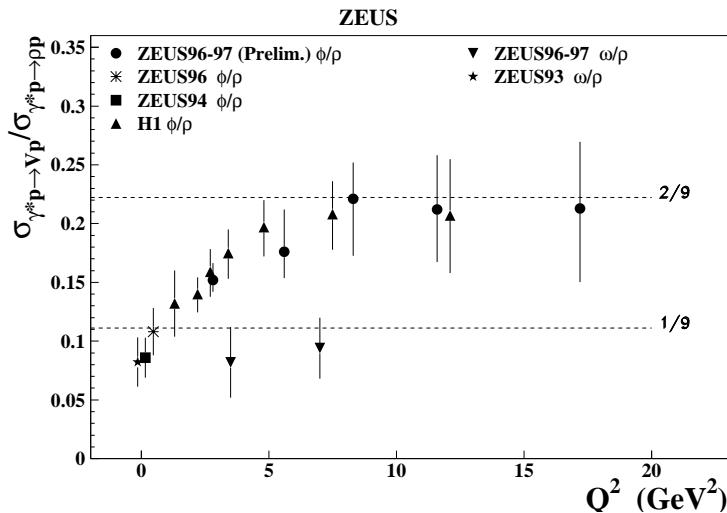
The ratio of  $\phi$  to  $\rho^0$  elastic electroproduction is shown in Fig. 5 [14]. Of particular interest is the observation that the  $Q^2$  dependence for these two vector mesons becomes similar at the same scale at which the cross section ratio reaches the value obtained from simple quark-charge counting. Since the ratio  $R$  for the  $\phi$  is known to exhibit a  $Q^2$  dependence similar to that for the  $\rho^0$  [10], we can conclude that  $\sigma_L$  and  $\sigma_T$  show a hard scaling behavior for the  $\phi$  as well, and that the observed scaling is a property of the vacuum-exchange process little modified by meson binding effects.



**Figure 3.** Ratio of the longitudinal and transverse elastic  $\rho^0$  electroproduction cross sections,  $R = \sigma_L/\sigma_T$ , as a function of  $Q^2$ . The solid line shows the result of a fit to the form  $R = (Q^2/M_\rho^2)^\kappa/\xi$ .



**Figure 4.** The longitudinal and transverse elastic  $\rho^0$  electroproduction cross sections as a function of  $Q^2$ . The solid lines shows the result of fits to the form  $(Q^2 + M_\rho^2)^{-n}$ .



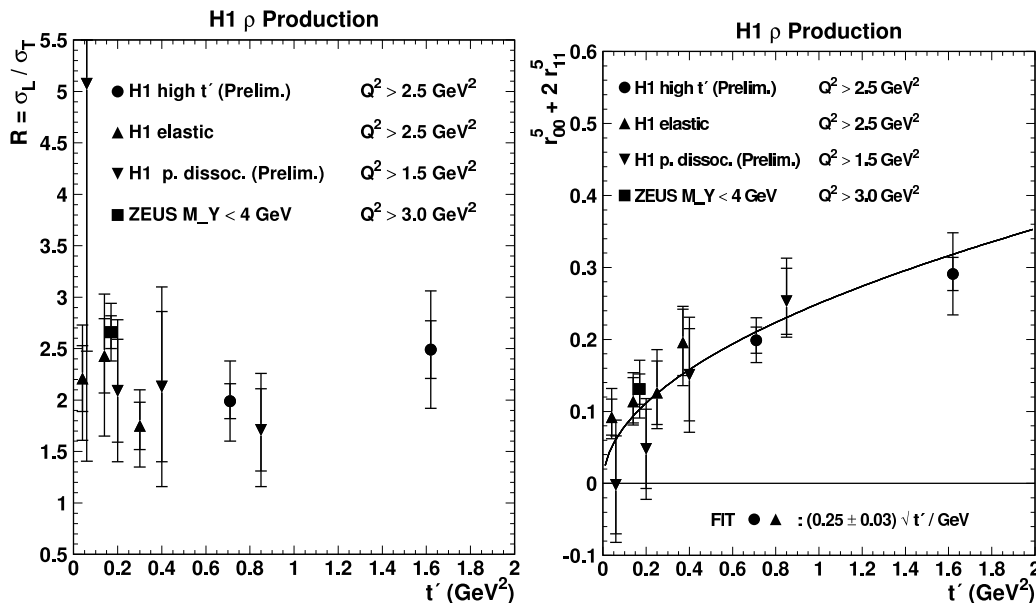
**Figure 5.** Ratios of the  $\phi$  and  $\omega$  elastic electroproduction cross sections to that for the  $\rho^0$  as a function of  $Q^2$ . The lines indicate the values for the ratios derived from the quark-charge content of the vector mesons.

Figure 5 also shows that the  $\omega/\rho^0$  ratio, which reached the value derived from quark-charge counting at low  $Q^2$ , does not rise with  $Q^2$  in this range. One can conclude either that some  $\phi$  suppression mechanism is active at low  $Q^2$ , or that there is an additional production mechanism which is similar for the  $\rho^0$  and  $\omega$  at low  $Q^2$  but absent in the case of the  $\phi$ .

The H1 collaboration has investigated the dependence of the ratio  $R$  and the combination of spin-density matrix elements  $r_{00}^5 + r_{11}^5$  on the momentum transfer to the proton [15]. Figure 6 shows the dependence on  $t'$ , which denotes the momentum transferred to the proton after subtraction of the kinematic lower bound. The ratio  $R$  shows no strong dependence on  $t'$  for  $Q^2$  greater than a few GeV<sup>2</sup>. The sum  $r_{00}^5 + r_{11}^5$  must vanish for  $s$ -channel amplitudes which conserve helicity [16] in the photon/vector-meson transition. Such conservation of helicity is a simple consequence of angular momentum conservation at zero momentum transfer. These results show evidence for a nonzero contribution from helicity-violating amplitudes which increases with  $t'$ .

### 3. The Pomeron trajectory measured in $\rho^0$ electroproduction

The ZEUS collaboration has extracted a measurement of the Pomeron trajectory in  $\rho^0$  electroproduction at  $Q^2$  values of 3.5 and 10.0 GeV<sup>2</sup> by measuring the energy dependence of the elastic cross section in four bins of  $t$  up to a value of 0.6 GeV<sup>2</sup> [9]. They find a value for the intercept of  $\alpha_{\mathbb{P}}(t=0) = 1.14 \pm 0.01(\text{stat}) \pm 0.03(\text{sys})$  and a slope of  $\alpha'_{\mathbb{P}} = 0.04 \pm 0.07(\text{stat})_{-0.04}^{+0.13}(\text{sys})$ . One can conclude that the trajectory for this process has a higher intercept and less shrinkage than the soft Pomeron trajectory which successfully describes hadronic cross sections at low momentum transfer.



**Figure 6.** Ratio of the longitudinal and transverse  $\rho^0$  electroproduction cross sections,  $R = \sigma_L / \sigma_T$ , and the combination of spin-density matrix elements  $r_{00}^5 + r_{11}^5$  as a function of  $t'$ .

#### 4. Vector-meson photoproduction at high momentum transfer

The ZEUS collaboration has extended its previous measurement of proton-dissociative vector-meson photoproduction [17] to higher momentum transfer ( $|t| \lesssim 11 \text{ GeV}^2$ ) by exploiting the higher statistics of the data set recorded in 1996/1997 [18]. A small electron calorimeter positioned near the electron beam-pipe 44 m from the interaction point served to select events initiated by quasi-real photons in the process  $\gamma + p \rightarrow \text{VM} + Y$ , where  $Y$  represents a dissociated state of the proton. The resulting range in  $\gamma p$  center-of-mass energy extends from 80 to 120 GeV. Since the transverse momentum of the final-state positron was required to be small by the geometrical acceptance of the calorimeter ( $Q^2 < 0.02 \text{ GeV}^2$ ), the transverse momentum of the vector meson,  $p_t$ , provided an accurate estimate of the square of the momentum transferred to the proton via  $t \simeq -p_t^2$ . The differential cross sections  $d\sigma/dt$  were obtained in the region  $|t| > 1.2 \text{ GeV}^2$  and are shown in Fig. 7. The measurements provide good sensitivity to the observed power-law dependence  $d\sigma/dt \propto (-t)^{-n}$  [19]. Over the region in momentum transfer covered by the data, the power is found to be  $n = 3.31 \pm 0.02(\text{stat}) \pm 0.12(\text{sys})$  for the  $\rho^0$  and  $n = 2.77 \pm 0.07(\text{stat}) \pm 0.17(\text{sys})$  for the  $\phi$  [18].

Figure 8 shows the ratio of  $\rho^0$  and  $\phi$  cross sections as a function of  $t$ . Just as in the case of electroproduction, one observes that the momentum-transfer dependence for these two vector mesons becomes similar at the same scale at which the cross section ratio reaches the value obtained from quark-charge counting. Such an observation yields valuable information concerning the nature of the short-distance coupling which is free of the large uncertainties arising from meson-binding effects in calculations of the absolute magnitudes of the cross sections.

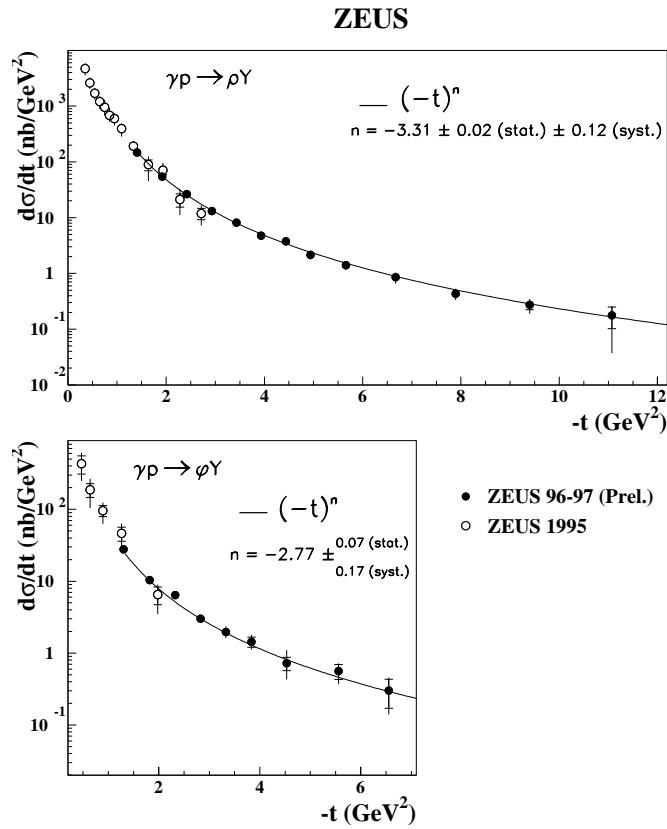


**Figure 7.** Differential cross sections  $d\sigma/dt$  for proton-dissociative photoproduction of  $\rho^0$  and  $\phi$  mesons. The open circles show the results of Ref. [17]. The lines show the results of fits of the form  $d\sigma/dt \propto (-t)^{-n}$  to the solid circles.

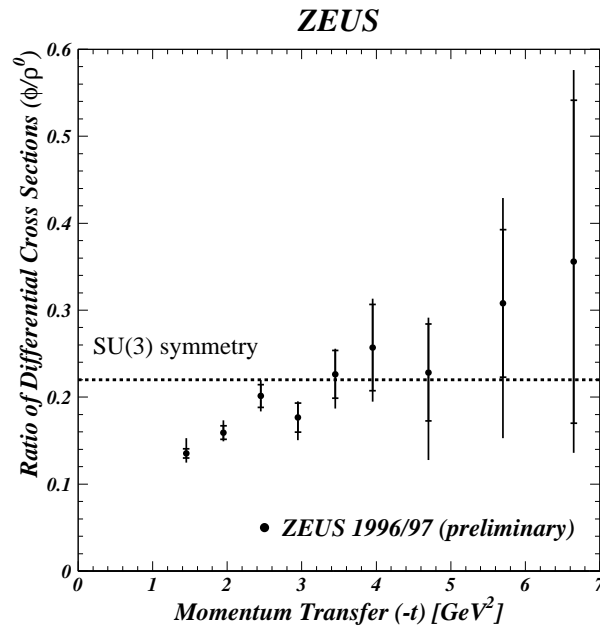


**Figure 8.** Ratio of the differential cross section  $d\sigma/dt$  for proton-dissociative  $\phi$  photoproduction to that for the  $\rho^0$  as a function of  $t$ . The line indicates the value for the ratio derived from the quark-charge content of the vector mesons.



Figure 9 shows the values for the combinations of spin-density matrix elements measured in the  $s$ -channel helicity frame  $r_{00}^{04}$ ,  $\text{Re } r_{10}^{04}$  and  $r_{1-1}^{04}$  as a function of  $t$  obtained from this data sample. The helicity-conserving (transverse-to-transverse) process clearly

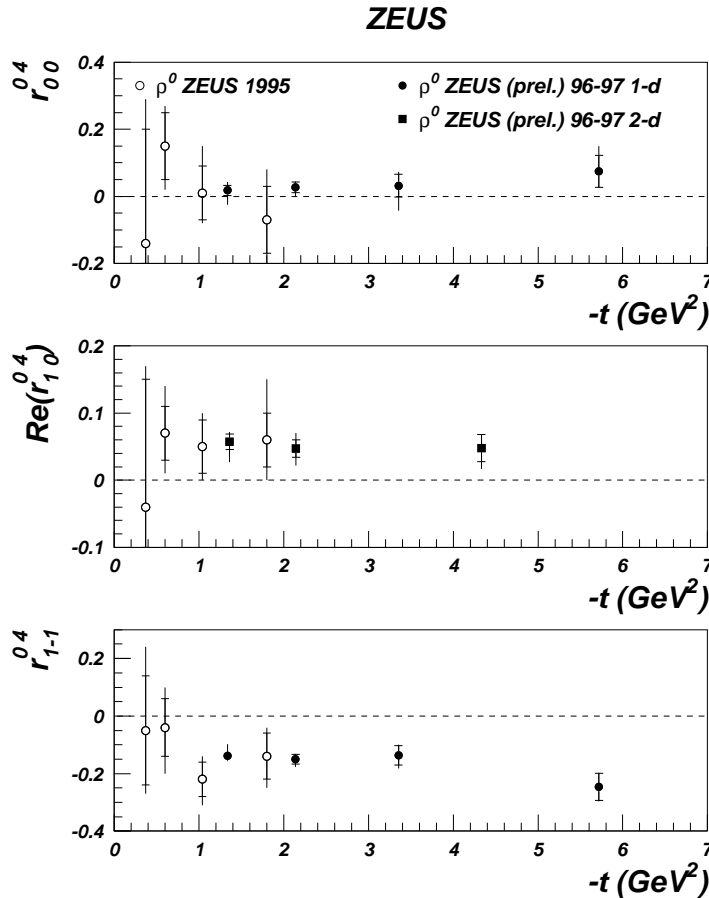


**Figure 9.** The values for the combinations of spin-density matrix elements  $r_{00}^{04}$ ,  $\text{Re } r_{10}^{04}$  and  $r_{1-1}^{04}$  for proton-dissociative  $\rho^0$  photoproduction derived from fits to decay-angle distributions, plotted as functions of  $t$ . The open circles indicate the measurements of Ref. [17].

dominates, as shown by the small value of  $r_{00}^{04}$ , which is the probability for longitudinal production, and by the small value of  $\text{Re } r_{10}^{04}$ , which is sensitive to the interference between the helicity-conserving ( $T \rightarrow T$ ) and single-flip ( $T \rightarrow L$ ) amplitudes. The statistical power of the data also allow accurate determination of a non-zero double-flip contribution, as shown by the non-zero value of  $r_{1-1}^{04}$  at high  $|t|$ , since it arises from the interference between the non-flip and double-flip amplitudes.

It should be noted that these results represent the first measurements of light-vector-meson photoproduction at values of  $t$  comparable to those of  $Q^2$  in inclusive deep inelastic electron-proton scattering which revealed the existence of fractionally charged proton constituents at SLAC in 1967. In contrast to the deep inelastic scattering process, this vacuum-exchange reaction is presumably sensitive to strong couplings rather than to the electric charges of the proton constituents. A transition to power-law scaling is

observed, and the momentum-transfer dependence for the  $\rho^0$  becomes similar to that for the  $\phi$  at the same scale at which the cross section ratio reaches the value obtained from quark-charge counting. Since this is also the region in which the momentum transfer exceeds the masses, one can plausibly assume that the observed dependence characterizes the underlying dynamics independent of meson-binding effects. Given the phenomenological successes of QCD descriptions of diffractive electroproduction of longitudinal vector mesons during the past few years, it is remarkable that the observed power for the dominant transverse-to-transverse amplitude in photoproduction is lower than expected from two-gluon-exchange calculations [7]. These calculations yield a leading  $(-t)^{-4}$  dependence, further steepened by the running of the strong coupling constant:  $d\sigma/dt \propto \alpha_s^4/(-t)^4$ . It is interesting to note that this expectation for the leading power behavior is not specific to QCD. Chernyak and Zhitnitsky have pointed out, for example, that these rules hold for the exchange of any vector or axial-vector current or for any Lagrangian with dimensionless coupling constants [2].

## 5. Conclusions

Investigations of the diffractive production of light vector mesons at HERA provide detailed information on the dynamics which govern vacuum-exchange processes. The dependence on proton-dissociation of the helicity-transfer properties of the virtual-photon/vector-meson transition has been shown to be weak, supporting the characterization of vector-meson electroproduction in this kinematic region as a diffractive process. A Pomeron trajectory has been measured in exclusive  $\rho^0$  electroproduction at high photon virtuality for the first time. This trajectory exhibits a higher intercept and weaker slope than does the trajectory measured in  $\rho^0$  photoproduction, which was similar to that determined in soft hadronic processes.

High-statistics measurements at values of both  $Q^2$  and  $t$  far exceeding the light-meson mass scale have been obtained. The expectation that meson-binding effects are small in this region are supported by the observation that the momentum-transfer dependence for the  $\rho^0$  becomes similar to that for the  $\phi$  at the same scale at which the cross section ratio reaches the value obtained from quark-charge counting. The common power behavior may thus be interpreted as characterizing the vacuum-exchange dynamics alone.

Decay-angle analyses have experimentally distinguished the momentum-transfer scaling properties of the various helicity amplitudes. The  $Q^2$  dependence for the longitudinal elastic  $\rho^0$  electroproduction has been found to follow a power law with a power approximately one unit lower than observed for the transverse cross section, as expected on very general theoretical grounds. However, results on the semi-exclusive photoproduction of  $\rho^0$  and  $\phi$  mesons at high momentum transfer show a remarkably hard power law to govern the short-distance transverse-to-transverse vacuum-exchange amplitude. The fundamental nature of the theoretical basis which leads to the expectation of a softer spectrum is likely to motivate an intensification of the already

widespread phenomenological activities which address the many experimental results on the diffractive production of vector mesons at HERA.

## 6. Acknowledgments

This work is supported by the Federal Ministry for Education and Research of Germany.

## References

- [1] S.J. Brodsky and G.P. Lepage, *Phys. Rev.* **D22**, 2157 (1980).
- [2] V.L. Chernyak and A.R. Zhitnitsky, *Phys. Rep.* **112**, 173 (1984).
- [3] S.J. Brodsky et al., *Phys. Rev.* **D50**, 3134 (1994).
- [4] J.C. Collins, L. Frankfurt and M. Strikman, *Phys. Rev.* **D56**, 2982 (1997).
- [5] D.Yu. Ivanov, *Phys. Rev.* **D53**, 3564 (1996).
- [6] I.F. Ginzburg and D. Yu. Ivanov, *Phys. Rev.* **D54**, 5523 (1996).
- [7] D.Yu. Ivanov, R. Kirschner, A. Schaefer and L. Szymanowski, *Phys. Lett.* **B478**, 101, erratum (2000).
- [8] M. Diehl, these proceedings.
- [9] ZEUS Coll., J. Breitweg et al., submitted to EPS-HEP01 in Budapest, abstract 594, 2001.
- [10] H1 Coll., C. Adloff et al., *Phys. Lett.* **B 483**, 360 (2000).
- [11] ZEUS Coll., J. Breitweg et al., Paper 439 submitted to the XXX Int. Conf. on High Energy Physics, 27 July - 2 August, 2000, Osaka, Japan.
- [12] A.D. Martin, M.G. Ryskin, and T. Teubner, *Phys. Rev.* **D55**, 4329 (1997);  
D.Yu. Ivanov and R. Kirschner, *Phys. Rev.* **D58**, 114026 (1998).
- [13] ZEUS Coll., J. Breitweg et al., *Eur. Phys. J.* **C12**, 393 (2000);  
H1 Coll., C. Adloff et al., *Eur. Phys. J.* **C10**, 373 (1999).
- [14] A. Kreisel for the ZEUS Coll., talk held at the 9th International Workshop on Deep Inelastic Scattering and QCD (DIS01), Bologna, Italy, May 2001;  
ZEUS Coll., J. Breitweg et al., Paper submitted to the XXIX International Conference on High Energy Physics, 23-29 July 1998, Vancouver, Canada (Abstract 793).
- [15] H1 Coll., C. Adloff, et al., submitted to EPS-HEP01 in Budapest, abstract 796, 2001.
- [16] K. Schilling and G. Wolf, *Nucl. Phys.* **B61**, 381 (1973).
- [17] ZEUS Coll., J. Breitweg et al., *Eur. Phys. J.* **C14**, 213 (2000).
- [18] ZEUS Coll., J. Breitweg et al., submitted to EPS-HEP01 in Budapest, abstract 556, 2001.
- [19] J.A. Crittenden, in *Proceedings of DPF2000: The Meeting of the Division of Particles and Fields*. American Physical Society, Columbus, Ohio, USA, 2000, hep-ex/0010079.